



10-5-3

## VIBRATION TEST OF A MODEL OF NUCLEAR POWER PLANT USING A LARGE SHAKING TABLE (PART 2 BWR 1/12 SCALE MODEL)

Akiyoshi YANO<sup>1</sup> and Katsuihiro HIJIKATA<sup>1</sup>

<sup>1</sup> Tokyo Electric Power Company Limited, Chiyodaku, Tokyo, Japan

### SUMMARY

A vibration test of a scaled model of a nuclear power plant using a large shaking table was conducted to clarify an elasto-plastic response characteristics under the severe earthquake load. A Mark-II type reactor building was selected as a target of a specimen, then was simplified and scaled down to 1/12. A specimen was exposed from low to high intensity, and it was collapsed with a shear destruction. Through a successful analytical correlation by a conventional method, applied in a practical design of a nuclear power plant, a validity and an availability of a current design procedure was proved.

### INTRODUCTION

A dynamic test of a scaled model utilizing a large scale shaking table of Nuclear Power Engineering Test Center (NUPEC) in Japan was conducted to investigate an elasto-plastic response behavior of a reactor building under a design level or more severe earthquake excitation, which was designed using a current design method. Main objects of this research work are as follows:

- (1) To prove the soundness of the reactor building exposed to the design level earthquake;
- (2) To estimate the seismic safety margin of the reactor building against the destructive stage;
- (3) To prove a validity and an availability of the conventional analytical method through the simulation analysis of test results.

This paper is a summary of the cooperative research project of 10 Japanese electric companies, titled "Vibration Test of Model of Nuclear Power Plant Using A Large Shaking Table" (Ref.1.).

### TEST STRUCTURE

As the target of the test structure, A Mark-II of BWR type reactor was chosen. Considering the restriction for a shaking table test, the prototype of the test structure was determined through an idealization ignoring the soil-structure interaction, a reduction of stories and an elimination of irregularities and unsymmetries. The dimension of the test structure was determined with a following rules:

- (1) The test structure resembles to the prototype structure as much as possible, and has enough size to be excited to the destructive level;
- (2) As for the law of similarity, Cauchy's number ( $\rho V^2/E$ ) should be preserved, but Froude's number ( $V/\sqrt{Gl}$ ) will be relaxed.  $\rho$  is the density of materials, E is Young's modulus of materials, V is the velocity, G is the gravity and l is the length;
- (3) The thickness of slab was increased to be able to bear the weights, which were installed on each floor. The shape was simplified to make the construction of the test structure easy. A total weight of a test structure should be less than 500 tons considering the capacity of the lifting crane and the weight limitation of the shaking table.

The adopted law of similarity is summarized in Table 1 and the prototype structure, the plane and the sectional view of the test structure are shown in Fig.1.

**Fabrication of Test Structure** The shape of the test structure is so complex as shown in Fig.1 that it was difficult to cast the specimen at a time. The procedure adopted to construct the test structure as shown in Fig.2, are: (1) cast each wall independently; (2) cast a half bottom of the base mat, and install each wall on the correct position; (3) cast the upper part of the base mat; (4) cast the floor to connect three independent wall, after curing few days, weights are installed on the floor; (5) repeat the procedure (3) and (4) until the test structure is completed. The total weight of test structure is 486tons, 45% of the total weight is for weights and 30% for the mat slab.

As the thickness of wall is so thin (40—69mm), a special heat-treated deformed bars of which diameter was 5 and 6mm were used in the wall, and the micro concrete whose maximum aggregate size was less than 5mm was used for the walls. Mechanical properties of the materials are listed in Table 2.

**Test Program** An artificial earthquake motion ( $M=8.5$ , Distance=68km, Hachinohe Eq's Phase Angle and Maximum Acceleration=401.7Gal) was used for an input waveforms. The time-axis was scaled to  $1/4.38$  of the original according to the law of similarity. An input level was determined with reference to the result of the analytical prediction. The standard input level ( $A_0$ ) was 257Gal, which produces the response shear stress of  $24\text{kg/cm}^2$  ( $0.1F_c:F_c$  is the compressive strength of concrete) at the weakest part of the test structure, which is a 3rd floor of inner wall (IW3F). The input earthquake and its response spectrum are shown in Fig. 3. It is considered that the standard input level ( $A_0$ ) corresponds to the  $S_1$  earthquake motion defined in the process of the allowable stress level design of the actual reactor building. The input level was increased up to 9 times of the standard level of  $A_0$  as shown in a first column of table 3.

**Instrumentation** To grasp the behavior of the test structure, 238 points of instruments were used, which were 82 for the acceleration, 188 for the strain of reinforcements, 6 for the displacement, 12 for information from shaking table and 20 for others.

## TEST RESULTS

**Outline of Test** 9 levels of vibration tests ranging from the elastic stage to the ultimate stage were conducted. The maximum response values of typical tests were summarized in Table 3. It became difficult to control the shaking table as the increase of the input level, because of the non-linear behavior of the test structure. The level of the excitation was determined with the obtained acceleration value on the shaking table.

Reinforcements in the flange wall at IW3F yielded during the  $6A_0$  test. The inter-story drift of IW3F exceeded the pre-defined limit state value (6mm) during the  $9A_0$  test. It is judged that the test structure was collapsed. A crack pattern of the test structure after the  $2A_0$  and the  $9A_0$  tests are shown in Fig. 4.

**Dynamic Characteristics of Test Structure** An amplitude ratio, a natural frequency, a damping factor and a vibration mode of the test structure were examined. The amplitude ratio of the 6th floor level (corresponds to the operating floor) to the base mat was 6.1 in the elastic range. As the increase of the input level, it was changed and reduced to 5.7 on the  $A_0$  test and 2.6 on the  $9A_0$  test. The transfer function of the 6th floor to base mat on the  $A_0$  test is shown in Fig.5, two peaks of the 1st and the 2nd mode are clearly observed.

The relation between the shear stress of IW3F versus a natural frequency and a damping factor estimated from transfer functions on various tests with various method, are shown in Fig.6 and Fig.7 respectively. The natural frequency of the 1st mode of the test structure was 17.5Hz before the test, it decreased as the increase of the input level, for instance 15.2Hz on the  $0.5A_0$  test, 12Hz on the  $2A_0$  test and finally 4.3Hz on the  $9A_0$  test. This means the final stiffness decreased to 6% of the elastic stiffness. As for the damping factor of the 1st mode, until the  $A_0$  test, it was around 1 to 2%, then increased to 4% on the  $2.3A_0$  test and 6% on the  $4.5A_0$  test. The natural frequency of the 2nd mode was also decreased as the increase of the input level. The ratio of natural frequency of the 1st and the 2nd mode did not fluctuate so much. The damping factor of the 2nd mode was almost same values as that of the 1st mode. There was no special tendency like a viscous damping characteristics.

The change of the vibration mode obtained from the transfer function of every measuring point on the 1st and the 2nd mode with the input level are shown in Fig.8. In case of the 1st mode, the displacement of the 1st and the 3rd floor became larger on the  $2A_0$  and the  $2.3A_0$  test. During the  $2.6A_0$  test, the displacement of the 2nd floor increased. As for the 2nd mode, a nodal point was between the 5th and the 6th floor during the elastic stage, which coincides with the analytical prediction well, and that nodal point was going down as the increase of the input level.

The shear stress on IW3F are given in the 5th column of table 3. The average shear stress of IW3F at the final, destructive stage was 77.6kg/cm<sup>2</sup>. That value exceeds the predicted ultimate stress value (62.7kg/cm<sup>2</sup>) by Yoshizaki formula (Ref.2) about 23 % .

## ANALYTICAL CORRELATION

The simulation analysis was conducted to clarify the validity and the availability of the analytical method commonly used in the practical design of the nuclear power plant.

**Analytical Model** The test structure was modeled using the conventional flexural shear model with the lumped mass system. The spring constants were estimated from the results of the material test as shown in table 2. The damping factor was derived from the test results as shown in Fig.7. The analytical model is 3 sticks and 13 lumped masses model as shown in Fig.9. Both a horizontal and a rotational acceleration time histories recorded on the base of the test structure were input simultaneously to that model. Analyzed cases are the 0.5Ao ,the Ao and the 2Ao test.

**Restoring Force Characteristics** The restoring force characteristics was represented as a tri-linear skeleton curve and a hysteresis loop as shown in Fig.10. A hysteresis rule for a flexural component is a peak oriented until the 2nd break point. After that, it has a stable loop of a parallelogram. A rule for a shear component is a peak oriented. The first break point of shear stress is represented as a formula :  $\sqrt{Fc(\sqrt{Fc} + \sigma)}$  ( $\sigma$  is the normal stress), the ultimate point was represented with Yoshizaki's formula (Ref.2). The damping factor was estimated from the test results referred to Fig.7, 2% for until the Ao test and 4% for the 2Ao test. It was given as a form of strain energy proportional type.

**Results of Analysis** Fig.11 shows a comparison of the vibration mode obtained from the transfer function on the low level test and analytical prediction. Both the 1st and the 2nd mode coincide well each other, it is confirmed that the analytical model represents the test structure well. The results of response analysis and test results are compared in from Fig.12 to Fig.14. Fig.12 shows the response acceleration time histories on the 6th floor. Fig.13 shows the fourier spectrum of the time histories and Fig.14 shows the distribution of maximum response values. The 0.5Ao tests is the elastic range. Response waveforms, fourier spectrums and the distribution of maximum response of analytical and test result coincide well. In the Ao test, the test structure was almost in the elastic range. The pattern of response waveform and a peak frequency in a fourier spectrum correspond well, but an amplitude of analysis is larger than the test result. The distribution of maximum response corresponds slightly well. In the 2Ao test, the test structure was in the plastic range. The correspondence of the response waveform is well. In the fourier spectrum, a transient peaks caused by the deterioration of the stiffness was observed, but the terminate frequency corresponds well. As for the distribution of maximum response, a pattern that the lower stories were damaged is simulated well.

## CONCLUDING REMARKS

Through the shaking table test and the simulation analysis of the scaled model of BWR reactor building, the following remarks are obtained:

- (1) A complicated structure like the reactor building was successfully modeled with the application of the law of similarity, and the test structure was fabricated with enough accuracy to assure the reliable test results.
- (2) The test structure was sound against the severe level of the excitation of which level was 6Ao. Finally, the test structure was collapsed with the shear destruction at the 9Ao test at the predicted weakest part of the test structure.
- (3) The fundamental dynamic characteristics of the test structure can be represented with the conventional analytical model.
- (4) The test results were well simulated until the elasto-plastic range with the analytical method which are conventionally used in the practical design of the reactor building. The validity and the availability of the current design method was confirmed.

## ACKNOWLEDGEMENT

The authors wish to express their appreciations to the research fellows of Hitachi Ltd., Kajima Corporation, Shimizu Construction Co., Ltd., Toshiba Co., Ltd. and Takenaka Komuten Co., Ltd., for their contribution to this project. Takenaka Komuten Co., Ltd. and Toshiba Co., Ltd. successfully constructed the test structure, Shimizu Construction Co., Ltd. prepared and conducted the shaking table test, Hitachi Ltd. and Kajima Corporation conducted the simulation analysis and Kajima Corporation managed the project successfully.

## REFERENCES

1. S. SETOGAWA et al, "Vibration Test of Model of Nuclear Power Plant USING A Large Vibration Table (part 1-9)". Summaries of Tech. Papers A.I.J. (1987)
2. S. YOSHIZAKI et al, "Ultimate Shear Strength of the Nuclear Power Plant Structure Wall with Multi Opening Holes", J.I.C. Vol.22 No.1 (1984)

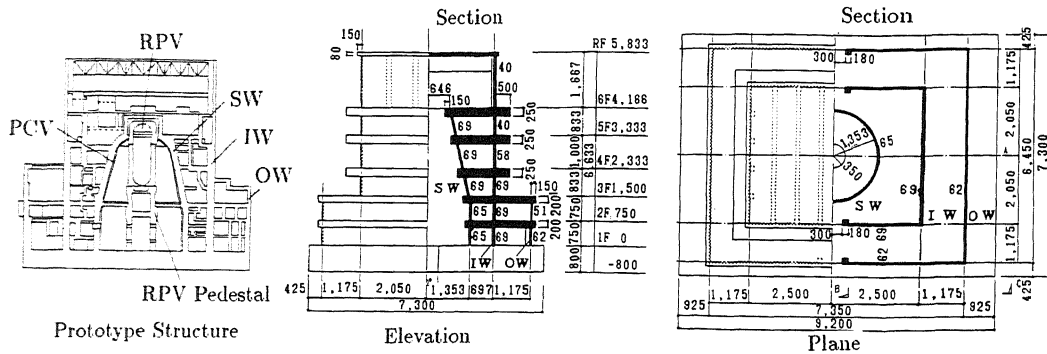


Fig.1 Test Structure

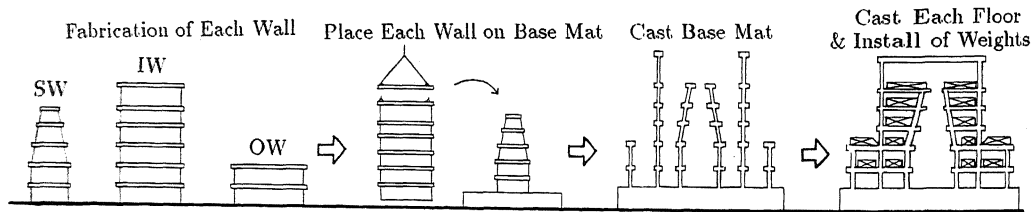


Fig.2 Procedure for Assembling Test Structure

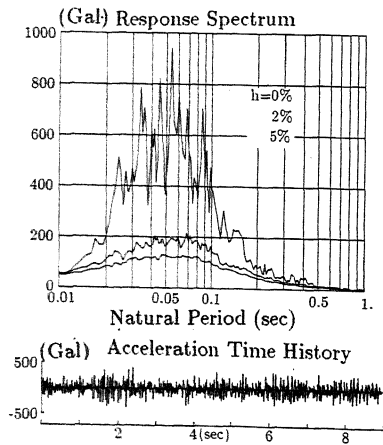


Fig.3 Input Earthquake Motion

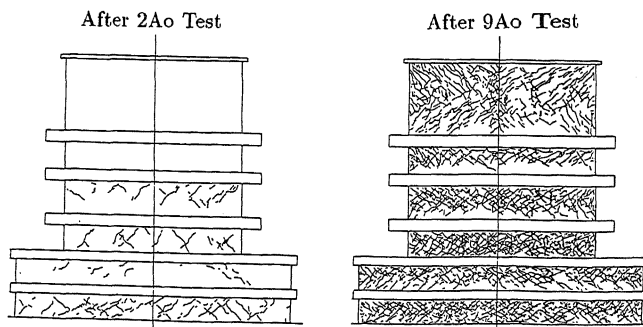


Fig.4 Crack Pattern of Test Structure

Table 1 The Law of Similarity

	Ratio (Model/Prototype)	
Length	$l/l$	$= 1/12$
Acceleration	$n$	$= 1.60$
Wall Thickness	$m$	$= 2.29$
Density	$l/(mn)$	$= 3.27$
Frequency	$\sqrt{nl}$	$= 4.38$

Table 2 Mechanical Properties of Materials  
(a) Reinforcing Bars

Diameter (mm)	Area (cm <sup>2</sup> )	Yield Point (kg/cm <sup>2</sup> )	Es (10 <sup>5</sup> kg/cm <sup>2</sup> )
D5	0.21	4700	1.97
D6(1)	0.30	3170	1.88
D6(2)	0.30	3620	1.92

(b) Concrete

Position	Strength (kg/cm <sup>2</sup> )		Ec (10 <sup>5</sup> kg/cm <sup>2</sup> )
	Compressive	Tensil	
outer wall	318	25.8	1.75
1,2F	289	22.7	1.66
Inner 3F	333	—	1.78
Wall 4F	323	26.4	1.94
5F	304	28.7	1.80
6F	278	—	1.63
Shield 1-3F	269	—	1.53
Wall 4-5F	263	21.4	1.51

Es and Ec is Young's Modulus of Material

Table 3 Maximum Response Values

Input Level	Base Acc. (Gal)	6F Acc. (Gal)	Shear (3F) (ton)	Shear Stress 3F (kg/cm <sup>2</sup> )	Rel. Disp. 3F (mm)
0.2Ao	38.5	254.7	28.1	4.0 <sup>*1</sup>	0.067
0.5Ao	137.4	755.3	83.8	11.9 <sup>*1</sup>	0.214
Ao	256.5	1469.	159.9	22.6 <sup>*1</sup>	0.439
2.0Ao	567.4	2303.	252.0	35.6 <sup>*1</sup>	0.966
2.3Ao	562.0	2409.	277.4	32.9 <sup>*2</sup>	1.355
2.6Ao	671.4	2371.	279.9	33.2 <sup>*2</sup>	1.231
4.5Ao	1228.0	3910.	370.4	44.0 <sup>*2</sup>	2.461
6.0Ao	1392.0	4340.	412.3	49.0 <sup>*2</sup>	2.564
9.0Ao	2633.0	6730.	654.3	77.6 <sup>*2</sup>	7.689

An ultimated Shear Stress by Yoshizaki's formula is 62.7kg/cm<sup>2</sup>

<sup>\*1</sup> Shear Stress of 3rd Floor of Inner Wall

<sup>\*2</sup> Average Shear Stress of Inner And Shield Wall

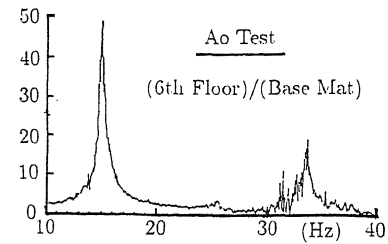


Fig.5 Transfer Function on Ao test

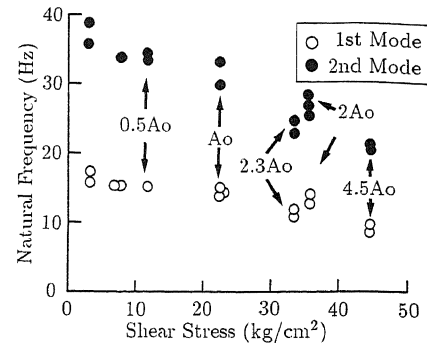


Fig.6 Deterioration of Test Structure  
(Natural Frequency Vs Shear Stress at IW3F)

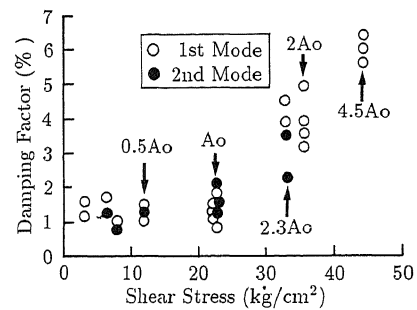


Fig.7 Deterioration of Test Structure  
(Damping Factor Vs Shear Stress at IW3F)

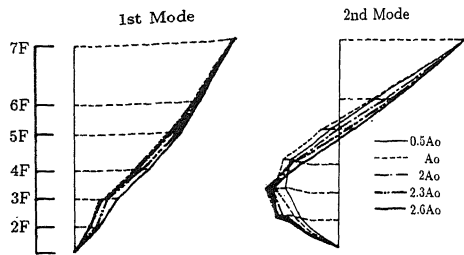


Fig. 8 Change of Vibration Mode

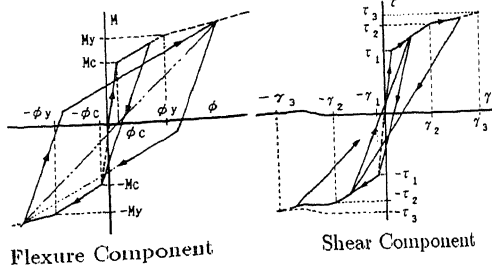


Fig. 10 Restoring Force Characteristics

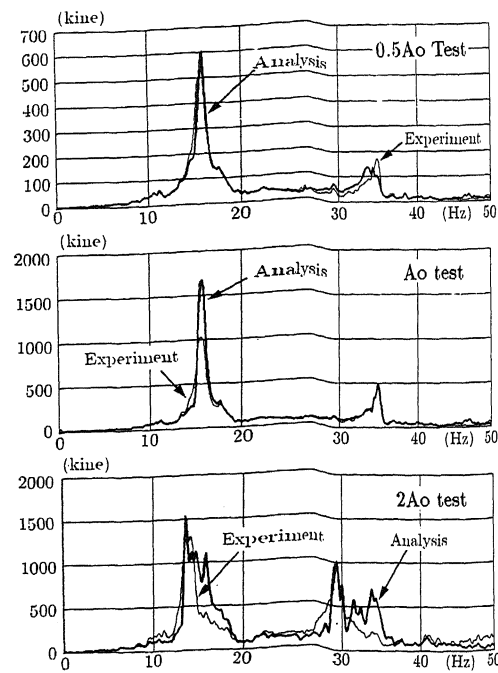


Fig. 13 Comparison of Fourier Spectrum of 6th Floor Response

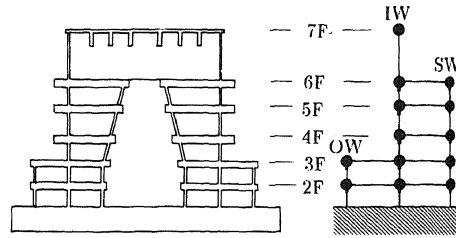


Fig. 9 Analytical Model

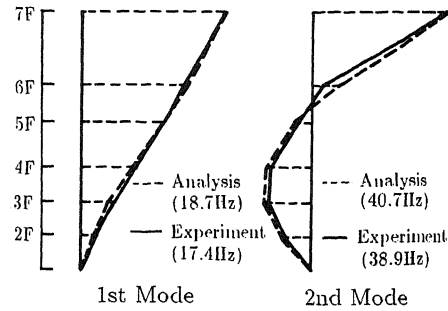


Fig. 11 Comparison of Vibration Mode

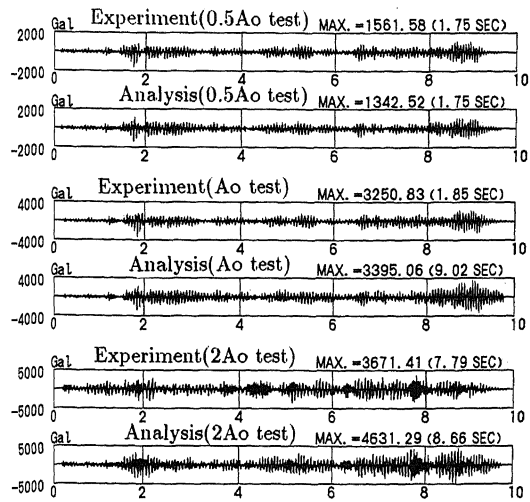


Fig. 12 Comparison of Response Waveform at 6th Floor

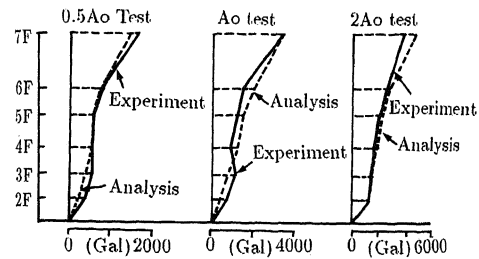


Fig. 14 Comparison of Distribution of Maximum Response Values